

# CRISPR–Cas9-assisted recombineering in *Lactobacillus reuteri*

Jee-Hwan Oh and Jan-Peter van Pijkeren\*

Department of Food Science, 1605 Linden Dr, University of Wisconsin-Madison, Madison, WI 53706, USA

Received April 15, 2014; Revised June 26, 2014; Accepted June 27, 2014

## ABSTRACT

**Clustered regularly interspaced palindromic repeats (CRISPRs) and the CRISPR-associated (Cas) nuclease protect bacteria and archaea from foreign DNA by site-specific cleavage of incoming DNA. Type-II CRISPR–Cas systems, such as the *Streptococcus pyogenes* CRISPR–Cas9 system, can be adapted such that Cas9 can be guided to a user-defined site in the chromosome to introduce double-stranded breaks. Here we have developed and optimized CRISPR–Cas9 function in the lactic acid bacterium *Lactobacillus reuteri* ATCC PTA 6475. We established proof-of-concept showing that CRISPR–Cas9 selection combined with single-stranded DNA (ssDNA) recombineering is a realistic approach to identify at high efficiencies edited cells in a lactic acid bacterium. We show for three independent targets that subtle changes in the bacterial genome can be recovered at efficiencies ranging from 90 to 100%. By combining CRISPR–Cas9 and recombineering, we successfully applied codon saturation mutagenesis in the *L. reuteri* chromosome. Also, CRISPR–Cas9 selection is critical to identify low-efficiency events such as oligonucleotide-mediated chromosome deletions. This also means that CRISPR–Cas9 selection will allow identification of recombinant cells in bacteria with low recombineering efficiencies, eliminating the need for ssDNA recombineering optimization procedures. We envision that CRISPR–Cas genome editing has the potential to change the landscape of genome editing in lactic acid bacteria, and other Gram-positive bacteria.**

## INTRODUCTION

Lactic acid bacteria (LAB) are a genetically and ecologically diverse group of Gram-positive bacteria encompassing 31 genera (1). There is a long history of the application of LAB in a variety of fermentation processes, but especially in the last three decades interest in LAB has significantly increased

since many strains, mostly members of the genus *Lactobacillus*, have health-promoting properties (2–5). In addition, many LAB strains are robust organisms that are able to withstand harsh conditions such as ethanol and stomach acid, which makes them attractive vehicles for the development of industrial producer strains and biotherapeutics, respectively (6–14). Taken together, LAB are therefore the most abundant group of Gram-positive bacteria used in industry and medicine representing a major economic factor.

For bacterial strains that are of industrial and medical importance, it is key that their genomes can be efficiently edited. This allows improvement of microbial strains in a timely manner, and will enhance our understanding how health-promoting bacteria elicit their effects. In various LAB, mutations can be generated in the chromosome by single-stranded DNA (ssDNA) recombineering (15,16). ssDNA recombineering requires inducible expression of a phage-derived ssDNA-binding protein (RecT or Beta), and an oligonucleotide that is identical, other than the base changes that need to be made, to the lagging strand of replication (17–20). Once the oligonucleotide is in the cell, the ssDNA-binding protein protects the oligonucleotide from degradation by host nucleases and aids to form a complex between the oligonucleotide and the lagging strand template DNA. An annealed oligonucleotide may serve as a primer for replication, which can be extended into a new daughter strand by DNA polymerase (18,21). The efficacy with which the oligonucleotide is incorporated is strongly dependent on the bacterial host, the activity of the phage-derived ssDNA-binding protein and ability of mismatches generated to evade the host mismatch repair system (15,22–24). Establishing ssDNA recombineering in a new species is not trivial, exemplified by the fact that there are few strains where mutations can be generated in the absence of selection (15,16,20). Thus, the ability to genetically engineer bacterial genomes by ssDNA recombineering at high efficiencies is a major bottleneck when establishing this technology. Recently, in *Escherichia coli*, ssDNA recombineering was combined with the type-II clustered regularly interspaced short palindromic repeats (CRISPRs) and CRISPR-associated (Cas) nuclease system of *Streptococcus pyogenes* to eliminate cells whose genomes have not been edited (25).

\*To whom correspondence should be addressed. Tel: +1 608 890 2640; Fax: +1 608 262 6872; Email: vanpijkeren@wisc.edu

CRISPR–Cas system can be regarded as an immune system for the bacteria and archaea as it efficiently cleaves foreign DNA entering the cell, such as phage or plasmids (26,27). Short DNA target sequences are located between the CRISPR repeats making up a CRISPR-array of targets. The CRISPR-array is transcribed and processed within the repeat sequences yielding RNA fragments, called CRISPR-RNA (crRNA). The crRNA serves to direct the Cas nuclease to the target site, and the presence of a specific protospacer-adjacent motif (PAM) results in Cas9-mediated cleavage of the target sequence. In type-II CRISPR–Cas systems, Cas9 will form a dual-RNA complex as Cas9 complexes with crRNA and a trans-activating CRISPR RNA (tracrRNA) that is required for Cas9 nuclease activity. The crRNA can be homed to user-defined locations in the genome to promote double-stranded breaks to eliminate unedited DNA (25,28–30).

This study describes the development and optimization of CRISPR–Cas9 selection in *Lactobacillus reuteri* ATCC PTA 6475, a strain with probiotic properties (31–35). We combined CRISPR–Cas9 with ssDNA recombineering to remove unedited cells from the population (Figure 1). We show that CRISPR–Cas9-assisted selection also allows identification of low-efficiency events such as oligonucleotide-mediated deletions, and proves an efficient approach for targeted codon saturation mutagenesis. A variety of applications of CRISPR–Cas9 in LAB are discussed.

## MATERIALS AND METHODS

### Bacterial strains, plasmids and media

All bacterial strains and plasmids used in this study are listed in Supplementary Table S1. Lactobacilli and their derivatives were cultured at 37°C under hypoxic conditions (5% CO<sub>2</sub>, 2% O<sub>2</sub>) in deMan Rogosa Sharpe (MRS) medium (Difco; BD BioSciences). *Lactococcus lactis* NZ9000 was used as a general cloning host, cultured statically at 30°C in M17-broth (Difco; BD BioSciences) supplemented with 0.5% (w/v) glucose. Electrocompetent cells of the LAB used in this study were prepared as described before (36–38). When needed, antibiotics were supplemented at the following concentrations: 5 µg/ml erythromycin and chloramphenicol for *L. reuteri* ATCC PTA 6475 and *L. lactis* strains, and 25 and 10 µg/ml tetracycline for *L. reuteri* and *L. lactis*, respectively.

### Reagents and enzymes

All modification enzymes were purchased from Fermentas. Enzyme mixes for Gibson assembly were prepared in a manner identical to that previously described (39). Polymerase chain reaction (PCR) amplifications for cloning purposes were performed with Phusion Hot Start II Polymerase (Fermentas), and PCR amplifications for screening purposes were performed with Taq DNA Polymerase (Denville Scientific). Pellet Paint Co-Precipitant (Novagen) was used to concentrate DNA for Gibson assembly or conventional T4 DNA ligase cloning. Oligonucleotides were purchased from Integrated DNA Technologies.

### Construction of vectors for CRISPR–Cas9 selection in *L. reuteri* 6475

All oligonucleotides can be found in Supplementary Table S2. pCAS9 and pCRISPR, both kindly provided by Luciano Maraffini (The Rockefeller University, New York, USA), were used as template DNA to construct derivatives for use in *L. reuteri*. The backbone of pNZ9530 was amplified with oVPL112–oVPL113 whereby the genes encoding NisR and NisK were excluded yielding a 4.8-kb fragment. The sequence containing the tracrRNA, *cas9* and the direct repeats was amplified from pCAS9 with oVPL114–oVPL115 (5-kb amplicon), whereby the resulting amplicon has on the proximal ends 40 bases complementary to the pNZ9530 amplicon generated by oVPL112–oVPL113. Amplicons were precipitated by Pellet Paint Precipitation, and quantified by Qubit Fluorometric Quantitation (Life Technologies). Both amplicons were fused by Gibson assembly, followed by transformation in *L. lactis* NZ9000. Fusion of both amplicons was confirmed by restriction digest analysis of plasmid DNA, followed by Sanger sequencing to confirm the integrity of the DNA sequence. The resultant construct was named pVPL3004.

For cloning the direct CRISPR repeats, we first constructed a derivative of pNZ8048 in which we replaced the gene coding chloramphenicol resistance (*cm*) with a gene coding tetracycline resistance (*tet*). This would allow us to use this vector in combination with vectors that encode erythromycin and chloramphenicol resistance. We amplified the backbone of pNZ8048 with oVPL362–oVPL363, located upstream and downstream, respectively, of the *cm* gene in pNZ8048. The *tet* gene was amplified with oVPL360–oVPL361 using pORI19Tet (kind gift from Robert Britton, Michigan State University) as template. Both amplicons were precipitated and quantified as described above, and mixed at a 1:1 molar ratio (vector:insert) followed by ligation and electroporation in *L. lactis* NZ9000. Plasmid DNA derived from tetracycline-resistant colonies was digested with NcoI, an enzyme that digests in the pNZ8048 multiple cloning site and internal to the tetracycline resistance gene, to confirm insertion. The resultant plasmid was named pVPL3112. We constructed a derivative of the RecT expression plasmid pJP042 in which we replaced the gene coding for erythromycin with a gene coding for chloramphenicol resistance to yield pVPL3017. The backbone of pJP042 and the *cm* gene were amplified with oVPL154–oVPL155 and oVPL156–oVPL157, respectively, and fused by Gibson assembly. The *recT* gene (locus tag HMPREF0536\_0521) is derived from a *L. reuteri* 6475 prophage (15).

Next, the backbone of pVPL3112 was amplified with oVPL309–oVPL310, and the direct CRISPR repeats were amplified with oVPL320–oVPL321. Both amplicons were precipitated and quantified as described above, followed by blunt-end ligation (1:1 molar ratio vector:insert). We confirmed by sequence analysis insertion of the CRISPR repeats yielding pVPL3115, which for clarity is also referred to as pCRISPR*ctrl*.

A derivative of pCRISPR*ctrl* was prepared to target the *lacL* locus in *L. reuteri* 6475 (see Supplementary Table S2 for oligonucleotides used). Briefly, pCRISPR*ctrl*

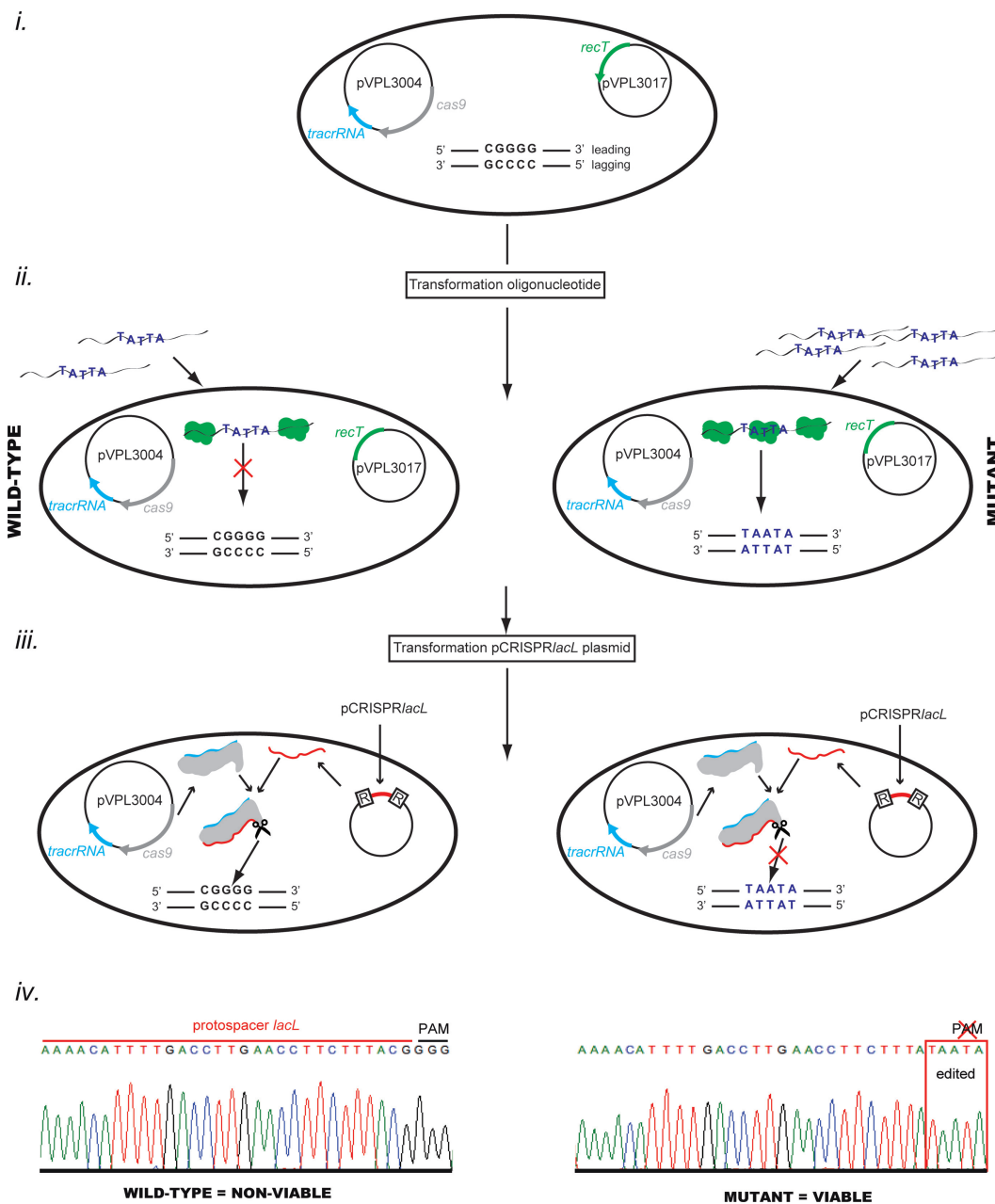


**Figure 1.** Overview of CRISPR–Cas9-assisted oligonucleotide genome editing in *Lactobacillus reuteri*. **(i)** *L. reuteri* 6475 (black oval) harbors pVPL3004 and pVPL3017, which code for the Cas9 nuclease and the *tracrRNA*, and RecT, respectively. Cas9 and the *tracrRNA* are constitutively expressed, but are for clarity not shown here. Part of the bacterial chromosome is represented by two black lines; on the right side the leading and lagging strand of replication is indicated. Central are five base pairs in *L. reuteri lacL*, which were targeted in this study by ssDNA recombineering. **(ii)** Electrocompetent cells are prepared in which RecT is expressed (green) after which 100 µg recombineering oligonucleotide, identical to the lagging strand of replication, is transformed in the cells. Oligonucleotides are depicted as wavy lines in which the five bases (5'-TATTA-3') indicate the desired mutations to be incorporated in the lagging strand of the *lacL* locus. Once oligonucleotides are in the cell, RecT proteins will bind to ssDNA molecules to protect them from degradation, and to aid to form a complex with the lagging template strand (not shown in figure). Left: in *L. reuteri*, ~95–99% of cells do not incorporate the oligonucleotide in the chromosome (indicated by red X) due to no, or insufficient oligonucleotide molecules entering the cell or suboptimal physiological conditions required for efficient oligonucleotide incorporation such as lower RecT levels. Cells with unedited chromosomes remain wild-type. Right: when the oligonucleotide is incorporated in the chromosome, five adjacent mutations are generated in the lagging strand, resulting in a pure genotype after chromosome and cell segregation. **(iii)** The population of cells now has a mixture of wild-type and mutant genotypes with abundance (95–99%) of wild-type cells. To select for cells in which the recombineering oligonucleotide is incorporated in the chromosome, pCRISPR*lacL* is transformed to allow for CRISPR–Cas9 selection. pCRISPR*lacL* encodes a CRISPR-array that is made up of direct repeats (indicated by boxed R) and the protospacer target sequence (indicated by red line in-between repeats). The Cas9 nuclease (gray) and *tracrRNA* (cyan), required for Cas9 to cleave the target DNA, form an active complex with the RNA target CRISPR-array sequence (red). Left: in wild-type cells, the dual-RNA Cas9 will bind the chromosomal target DNA sequence, and the *S. pyogenes*-derived Cas9 will efficiently cleave the host DNA if the PAM matches the consensus triplet NGG. **(iv)** The chromatogram shows more information on the DNA sequence composition. Cleavage of the chromosomes of unedited cells will eliminate the large wild-type population. Right: cells in which the oligonucleotide has been incorporated in the chromosome have the modified *lacL* target, including the PAM sequence, and hence the dual-RNA Cas9 complex will not be able to cleave the host DNA. This approach allows genome editing with minimum effort.

was digested with BsaI, which cleaves internal to the two CRISPR repeats, followed by gel purification (Fermentas gel purification kit). This allows cloning of a fragment with clamps complementary to the BsaI site to yield a plasmid that contains CRISPR-target sequence-CRISPR. To this end, a pair of complementary oligonucleotides (oVPL151-oVPL152), identical to the 30-bp *lacL* target region, were annealed generating a double-stranded fragment with overhangs complementary to pCRISPR<sub>ctrl</sub> digested with BsaI. DNA was mixed at a 1:1 molar ratio followed by overnight ligation, pellet paint precipitation and transformation in *L. lactis* NZ9000. We confirmed by sequence analysis insertion of the *lacL* protospacer, yielding pCRISPR<sub>lacL</sub>. In an analogous manner, we constructed pCRISPR<sub>srtA</sub> and pCRISPR<sub>sdp6</sub> by cloning the complementary oligonucleotides oVPL447-oVPL448 and oVPL453-oVPL454, respectively. The integrity of all pCRISPR plasmids constructed in this study was confirmed by sequence analysis.

### CRISPR-assisted oligonucleotide genome editing in *L. reuteri*

We established a single-step and a more robust dual-step approach for CRISPR-assisted oligonucleotide genome editing in *L. reuteri*, whereby we used the *lacL* gene (locus tag HMPREF0536\_0317), the *srtA* gene (locus tag HMPREF0536\_0973) and the *sdp6* gene (locus tag HMPREF0536\_0710) as targets to establish proof-of-concept. Cells harboring both pVPL3004 (expressing Cas9 and tracrRNA) and pVPL3017 (RecT expression plasmid) were made competent as previously described (15), with the exception that the growth media contained 5 µg/ml erythromycin and 5 µg/ml chloramphenicol. For the one-step procedure, cells were co-transformed with 100 µg recombineering oligonucleotide (oVPL153<sub>lacL</sub> or oVPL449<sub>srtA</sub> or oVPL455<sub>sdp6</sub>) and 100 ng of the corresponding pCRISPR<sub>target</sub> (pCRISPR<sub>lacL</sub> or pCRISPR<sub>srtA</sub> or pCRISPR<sub>sdp6</sub>, respectively). Each of the recombineering oligonucleotides was also combined with pCRISPR<sub>ctrl</sub>, which produces a crRNA that does not have homology to the *L. reuteri* chromosome. Each of the recombineering oligonucleotides changes upon incorporation five adjacent bases: oVPL153<sub>lacL</sub> (CGGGG to TAATA), oVPL449<sub>srtA</sub> (AAGGT to TGACA), oVPL455<sub>sdp6</sub> (GGCAG to CTAGC). The protospacer-adjacent site NGG is thus disrupted in all targets, and incorporation of each recombineering oligonucleotide yields in-frame stop codons (see Supplementary Table S1). The pCRISPR<sub>target</sub> plasmids will guide cleavage by Cas9 of the chromosomal target regions if these are not edited by each of the ssDNA recombineering oligonucleotides. After electroporation and recovery, cells were plated on MRS plates with double antibiotic selection to select for pVPL3004 (5 µg/ml erythromycin) and the pCRISPR plasmid (25 µg/ml tetracycline). Colonies were screened by mismatch amplification mutation assay-PCR (MAMA-PCR) (40). MAMA-PCR for the targets *lacL*, *srtA* and *sdp6* was performed with oligonucleotides oVPL347-oVPL348-oVPL349, oVPL468-oVPL469-oVPL470 and oVPL474-oVPL475-oVPL476, respectively.

For the dual-step procedure, cells were transformed with 100 µg oVPL153<sub>lacL</sub> followed by overnight recovery in 40 ml MRS harboring 5 µg/ml erythromycin. This overnight recovery step provides additional replication cycles during which oVPL153<sub>lacL</sub> can be incorporated in the chromosome, thereby generating a larger population of mutant genotypes. The next day cells were subcultured in MRS to OD<sub>600</sub> = 0.1 harboring 5 µg/ml erythromycin, and competent cells were prepared as described previously, but RecT was not induced prior to transformation. Competent cells were transformed with 100 ng pCRISPR<sub>lacL</sub> or pCRISPR<sub>ctrl</sub>, followed by 2-h recovery in MRS. Plating and screening were performed as described for the one-step procedure. Studies to generate deletions were performed with the dual-step procedure. For both the single-step and the dual-step approach, data were expressed as the level of tetracycline-resistant colony forming units (tet<sup>R</sup> cfu) per 10<sup>8</sup> viable cells. It needs to be noted that actual viability levels after electroporation and recovery ranged between 4 × 10<sup>8</sup> and 1 × 10<sup>9</sup> total cells.

### CRISPR-assisted targeted codon saturation mutagenesis

For codon saturation mutagenesis, a dual-step approach was performed as described above. The recombineering step was performed with 100 µg oVPL627<sub>NNK</sub>. Incorporation of this oligonucleotide yields a single base change (silent mutation) in the PAM region of *srtA*. Four adjacent mismatches (all silent mutations) are predicted to evade the mismatch repair system, and adjacent to these mismatches are bases that make up a degenerate codon (NNK; N = A/T/G/C, K = T/G). The NNK triplet can yield 32 different codons encompassing all 20 amino acids. In the second step, cells were transformed with 100 ng pCRISPR<sub>srtA</sub>. A total of 180 tetracycline-resistant colonies were screened by MAMA-PCR with oligonucleotides oVPL628-oVPL629-oVPL630. Wild-type genotypes yield a 600-bp fragment and incorporation of oVPL627<sub>NNK</sub> yielded a 300-bp fragment. Colonies yielding an amplicon of 300 bp were subjected to a second PCR with oligonucleotides oVPL468-oVPL469, and submitted for sequence analysis.

## RESULTS

### Establishing CRISPR–Cas9 activity in *L. reuteri* 6475

The goal of this study was to establish CRISPR–Cas9 selection in a lactic acid bacterium strain to allow high-efficiency fine-tuned genome editing. To demonstrate functional CRISPR–Cas9 activity in *Lactobacillus* cells expressing RecT, we used *L. reuteri* ATCC PTA 6475 as our model organism. Our approach was to establish *L. reuteri* cells that contain plasmids that produce RecT, key to ssDNA recombineering, and produce Cas9 along with *tracrRNA* which make up part of the CRISPR–Cas9 system. Recombineering oligonucleotides are introduced into cells along with a plasmid that produces an user-defined crRNA transcript, which complements the *tracrRNA* and Cas9 to eliminate cells in which the recombineering oligonucleotide was not incorporated in the chromosome.

To achieve this, we cloned DNA coding for Cas9 and the *tracrRNA* in the low-copy vector pNZ9530 yielding

pVPL3004, and established this plasmid in *L. reuteri* that already harbored pVPL3017, which codes for RecT. Subsequently, two plasmids, both coding for tetracycline resistance, were constructed that produce a CRISPR-array with no homology to the *L. reuteri* chromosome (pCRISPR $ctrl$ ), or with homology to the *L. reuteri* wild-type *lacL* locus (pCRISPR $lacL$ ). pCRISPR $ctrl$  does not target the *L. reuteri* chromosome and can be considered a control for transformation. pCRISPR $lacL$  will produce a CRISPR-array that together with Cas9 and the *tracrRNA* cleaves DNA in the *lacL* locus, unless it is edited by ssDNA recombineering by means of incorporation of oVPL153 $_{lacL}$ . oVPL153 $_{lacL}$  yields five adjacent mismatches, and based on previous studies we anticipate this will evade mismatch repair in *L. reuteri* 6475 (15,16).

Our first aim was to determine the efficacy of CRISPR–Cas9 selection in *L. reuteri* 6475 by comparing the number of transformants obtained from pCRISPR $ctrl$  to pCRISPR $lacL$  when combined with a control recombineering oligonucleotide. *L. reuteri* harboring pVPL3004 and pVPL3017 was made competent after induction of RecT and co-transformed with 100  $\mu$ g control oligonucleotide targeting *rpoB* (oVPL236 $_{rpoB}$ ) and 100 ng pCRISPR $ctrl$  or pCRISPR $lacL$ , respectively. We obtained  $5 \times 10^3$  tetracycline-resistant transformants when cells were co-transformed with oVPL236 $_{rpoB}$ +pCRISPR $ctrl$ . This transformation efficiency is 2 orders of magnitude lower compared to transformation efficiencies obtained with the same plasmid in *L. reuteri* 6475 wild-type cells (see Discussion). No transformants were obtained with oVPL236 $_{rpoB}$ +pCRISPR $lacL$  indicative of CRISPR–Cas9 selection (Figure 2a). To ensure that the presence of pVPL3004 and transformation of either CRISPR plasmid does not affect the recombineering efficiency, we assessed the level of rifampicin-resistant colonies. Incorporation of oVPL236 $_{rpoB}$  yields base changes in the RNA polymerase gene that result in amino acid changes that render the cells resistant to rifampicin. We recovered  $10^7$  rifampicin-resistant colonies per  $10^9$  viable cells (data not shown), similar to levels previously described for *L. reuteri* 6475 (15). Collectively, these data suggest that CRISPR–Cas9 efficiently cleaves *L. reuteri* 6475 chromosomal DNA, and does not affect the recombineering efficiency in this host.

### CRISPR–Cas selection post ssDNA recombineering increases the level of recombinants

To investigate whether we could combine Cas9 dual-RNA selection with ssDNA recombineering to recover mutant cells, we co-transformed 100  $\mu$ g oVPL153 $_{lacL}$  with 100 ng of pCRISPR $lacL$ . oVPL153 $_{lacL}$  yields five adjacent mismatches. Upon incorporation in the *lacL* locus, the PAM (Figure 1) is eliminated. Modification of the PAM site prevents the Cas9 dual-RNA complex-dependent cleavage of the host DNA at this locus, and survivor cells should have oVPL153 $_{lacL}$  incorporated in their DNA. After co-transformation of oVPL153 $_{lacL}$ +pCRISPR $lacL$ , we obtained on average a total of 27 tetracycline-resistant colonies per  $10^8$  viable cells (Figure 2a). Although this may suggest that recombinants are recovered, this level is

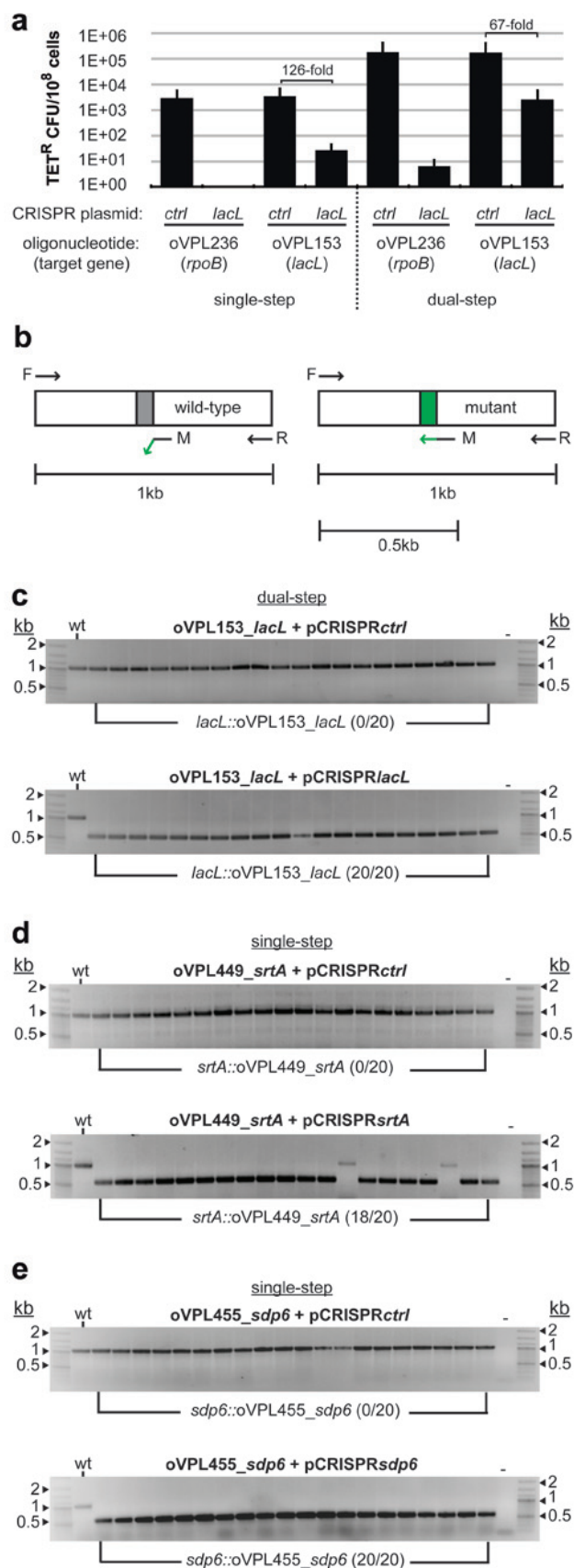


**Figure 2.** Efficient identification of recombinant cells by CRISPR–Cas9 genome targeting. (a) In the single-step procedure (left), *L. reuteri*

likely an underestimate since efficient oligonucleotide incorporation requires DNA replication; co-transformation of oVPL153\_ *lacL* and pCRISPR\_ *lacL* may therefore not yield enough replication cycles for oVPL153\_ *lacL* to be incorporated in the chromosome prior to Cas9-mediated DNA cleavage. To address this, we established a dual-step procedure where we first performed a ssDNA recombineering experiment followed by a second step with CRISPR–Cas9 selection. *L. reuteri* 6475 harboring pVPL3004 and pVPL3017 was transformed with 100 μg oVPL153\_ *lacL* or 100 μg control oligonucleotide, and cells were recovered overnight in 40-ml MRS. The next day competent cells were prepared, and cells initially transformed

harboring pVPL3004 (expressing Cas9 and tracrRNA) and pVPL3017 (expressing RecT) was co-transformed with 100 ng CRISPR-plasmid (pCRISPR\_ *ctrl* or pCRISPR\_ *lacL*) and 100 μg recombineering oligonucleotide targeting *rpoB* (oVPL236) or *lacL* (oVPL153). In the dual-step procedure (right), cells were first transformed with recombineering oligonucleotide, and the following day new competent cells were prepared and transformed with CRISPR-plasmid. The number of transformants obtained from pCRISPR\_ *ctrl* combined with oligonucleotide oVPL153\_ *lacL* or oVPL236\_ *rpoB* represents the transformation efficiency, whereas the number of transformants obtained from pCRISPR\_ *lacL* combined with oligonucleotide oVPL236\_ *rpoB* is representative for CRISPR–Cas9 selection. The level of transformants obtained from pCRISPR\_ *lacL* combined with oligonucleotide oVPL153\_ *lacL* represents the population of putative recombinants edited by the recombineering oligonucleotide. Results shown are averages of four independent experiments and error bars represent standard deviation of the mean values. Results are expressed as number of tetracycline-resistant colonies per 10<sup>8</sup> cells. (b) To identify recombinants, a MAMA-PCR was used. In wild-type cells (left), the forward (F) and reverse (R) oligonucleotide yield a 1-kb amplicon. The third oligonucleotide (M) has five bases on the 3'-end that are complementary to the bases incorporated by the recombineering oligonucleotide. In wild-type cells, these five bases are non-complementary to the template DNA and the DNA polymerase will not extend the MAMA oligonucleotide. In recombinant cells (right), the MAMA-oligonucleotide will be extended yielding a 0.5-kb amplicon. The bias in template availability may yield preferential amplification with abundance in 0.5-kb amplicons. (c) Twenty colonies derived from a dual-step CRISPR–Cas9-ssDNA recombineering experiment were screened by MAMA-PCR to identify recombinants in the *lacL* locus. A 1-kb fragment is indicative of a wild-type genotype, whereas the presence of a 0.5-kb fragment is indicative of a recombinant genotype. In the absence of CRISPR–Cas9 selection, (oVPL153\_ *lacL*+pCRISPR\_ *ctrl*) only 1-kb amplicons were obtained, indicating no colonies were identified in which oVPL153\_ *lacL* is integrated in the *lacL* locus (top gel). With CRISPR–Cas9 selection (oVPL153\_ *lacL*+pCRISPR\_ *lacL*), all 20 colonies yielded a 0.5-kb fragment, indicating that CRISPR–Cas9 successfully removed unedited cells from the population (bottom gel). Data shown are representative images from four independent experiments. (d) Twenty colonies derived from a single-step approach were screened by MAMA-PCR to identify recombinants in the *srtA* locus. In the absence of CRISPR–Cas9 selection (oVPL449\_ *srtA*+pCRISPR\_ *ctrl*), the lack of significant levels of a 500-bp amplicon suggested that no recombinants were obtained, as was confirmed by sequence analysis (top gel). With CRISPR–Cas9 selection (oVPL449\_ *srtA*+pCRISPR\_ *srtA*), 18 out of 20 colonies screened yielded a clear 500-bp amplicon. This, combined with sequence analysis confirmed a mutant genotype (bottom gel). (e) Twenty colonies derived from a single-step approach were screened by MAMA-PCR to identify recombinants in the *sdp6* locus. No recombinants were obtained in the absence of CRISPR–Cas9 selection (oVPL455\_ *sdp6*+pCRISPR\_ *ctrl*) as only 1-kb amplicons were obtained (top gel). With CRISPR–Cas9 selection (oVPL455\_ *sdp6*+pCRISPR\_ *sdp6*), all 20 colonies screened yielded a 500-bp amplicon indicative for a mutant genotype (bottom gel). Numbers on left and right side of the gel indicate fragment sizes in kilobases (kb); wt and – indicate that *L. reuteri* 6475 wild-type genomic DNA and water are used as template controls, respectively.

with either oligonucleotide were transformed in the second step with pCRISPR\_ *ctrl* or pCRISPR\_ *lacL*. Compared to the single-step procedure, the dual-step procedure increased, relative to pCRISPR\_ *ctrl*, the number of recombinants by 1.9-fold (Figure 2a). More importantly, a 100-fold higher transformation efficiency of pCRISPR\_ *ctrl* was obtained in cells transformed in the dual-step procedure compared to cells co-transformed with oligonucleotide and pCRISPR\_ *ctrl* (single-step; Figure 2a; see Discussion). This also dramatically increased the pool of potential recombinants as now more than 2,500 colonies are recovered from pCRISPR\_ *lacL* transformation, approximately 100-fold more compared to the co-transformation approach (Figure 2a). Consecutive transformation of oVPL236\_ *rpoB* and pCRISPR\_ *lacL* did yield several background colonies, which only could be present when the CRISPR system is evaded, however; background levels were only 0.25% compared with the dual-step transformation of oVPL153\_ *lacL* and pCRISPR\_ *lacL* (Figure 2a). To get an indication what percentage of tetracycline-resistant colonies are recombinants, we performed a MAMA-PCR screen (Figure 2b) (40). Only recombinants were recovered when cells were subjected to pCRISPR\_ *lacL* selection at a reproducible efficiency of 100% (Figure 2c). The mutant genotype was also confirmed by sequence analysis of amplicons derived from five randomly picked colonies that were positive by MAMA-PCR (data not shown).

Although the dual-step procedure provides a more robust approach to identify mutants, we assessed whether the few colonies obtained by a single-step approach yield similar efficiencies of recombinants. Only recombinants were recovered when cells were co-transformed with oVPL153\_ *lacL*+pCRISPR\_ *lacL*. We performed a MAMA-PCR screen on 20 tetracycline-resistant colonies, which yielded 100% efficiency. The mutant and wild-type genotypes of the *lacL* target region of five colonies derived from oVPL153\_ *lacL*+pCRISPR\_ *lacL* and oVPL153\_ *lacL*+pCRISPR\_ *ctrl*, respectively, were confirmed by sequence analysis (data not shown).

### Genome modification at different loci

To show that CRISPR–Cas9-assisted recombineering can be used to target loci other than *lacL*, we constructed two additional pCRISPR plasmids, pCRISPR\_ *srtA* and pCRISPR\_ *sdp6*. pCRISPR\_ *srtA* and pCRISPR\_ *sdp6* each produces a CRISPR-array that together with Cas9 and the tracrRNA cleaves within the sortase (*srtA*) locus, and a locus that encodes a surface protein (*sdp6*). Editing of *srtA* and *sdp6* by ssDNA recombineering by means of incorporation of oVPL449\_ *srtA* and oVPL455\_ *sdp6*, respectively, will eliminate the PAM by making five adjacent base changes and subsequently prevent cleavage by Cas9. Co-transformation of 100 μg oVPL449\_ *srtA*+100 ng pCRISPR\_ *srtA* and 100 μg oVPL455\_ *sdp6*+100 ng pCRISPR\_ *sdp6* yielded on average 60 and 18 tetracycline-resistant colonies per 10<sup>8</sup> viable cells, respectively (data not shown). We obtained 10<sup>3</sup> colonies per 10<sup>8</sup> cells with each of the recombineering oligonucleotides combined with pCRISPR\_ *ctrl*, comparable as observed with oVPL153\_ *lacL*+pCRISPR\_ *ctrl*. MAMA-PCR on colonies

derived from oVPL449\_srtA+pCRISPR<sub>ctrl</sub> yielded 1-kb amplicons, and a weak 500-bp fragment for all colonies screened, including wild-type, was obtained. Sequence analyses of 10 1-kb amplicons showed that all amplicons were wild-type, thus strongly suggesting that the 500-bp fragment was obtained from non-specific amplification of the MAMA-oligonucleotide. In two independent experiments, we obtained on average  $92.5 \pm 2.5\%$  recombinants when we screened 20 colonies derived from oVPL449\_srtA+pCRISPR<sub>srtA</sub> (Figure 2d). Similarly, we obtained  $95 \pm 5\%$  recombinants when screening 20 colonies derived from oVPL455\_sdp6+pCRISPR<sub>sdp6</sub>, whereas no recombinants were identified within the pool of cells derived from oVPL455\_sdp6+pCRISPR<sub>ctrl</sub> (Figure 2e). We obtained for each target five escaper colonies as determined by the co-transformation of the control oligonucleotide oVPL236\_rpoB combined with either pCRISPR<sub>srtA</sub> or pCRISPR<sub>sdp6</sub>. Thus, CRISPR-assisted oligonucleotide-mediated genome engineering functions at high efficiency in *L. reuteri* 6475. Both a single-step and a dual-step procedure yield 90–100% recombinants, but the dual-step procedure provides a more robust approach to identify recombinant cells.

### Low-frequency mutations can be recovered by CRISPR-assisted genome editing

Since Cas9 dual-RNA genome targeting provides strong selection in *L. reuteri* 6475, we tested whether CRISPR-Cas9-assisted genome editing also allows for identification of mutants that occur at lower frequencies, such as oligonucleotide-mediated chromosome deletions.

In *L. reuteri* 6475, oligonucleotide-mediated chromosome deletions larger than 250 bp occur at frequencies lower than 0.3% (unpublished observations). Here we establish that CRISPR-Cas9 selection can be used to select for low-efficiency events. 80-mer oligonucleotides were designed which, when incorporated in the chromosome, yield a 501-bp (oVPL489 $\Delta$ 501) or a 1002-bp (oVPL490 $\Delta$ 1002) in-frame deletion, thereby also deleting the protospacer sequence in the *lacL* locus (Figure 3a). The number of CRISPR escapers represents baseline levels of detection, and was determined by subsequent transformation of oVPL236\_rpoB and pCRISPR<sub>lacL</sub>. Based on three independent experiments, we obtained on average 97 escaper colonies within the pool of  $9 \times 10^8$  viable cells. Compared to these baseline levels, only an increase of 1.9-fold and 1.3-fold tetracycline-resistant colonies was obtained for oVPL489 $\Delta$ 501 and oVPL490 $\Delta$ 1002, corresponding respectively to 186 and 125 cfu. These data show that oligonucleotide-mediated deletions of ~0.5 and 1 kb are 100-fold less efficient compared to mutating five adjacent mismatches in the same locus, which corresponds to ~0.01% efficiency. Based on three independent experiments, a PCR screen on 46 tetracycline-resistant colonies with oligonucleotides that flank the deletion region (oVPL492-oVPL493) identified on average  $10 \pm 6$  and  $3 \pm 2$  deletion events of 0.5 and 1 kb, respectively (Figure 3b). In addition to *lacL*, we also successfully made an in-frame deletion of 702 bp in the *srtA* locus. Our approach was identical to that described for the deletions in the *lacL* locus with exception

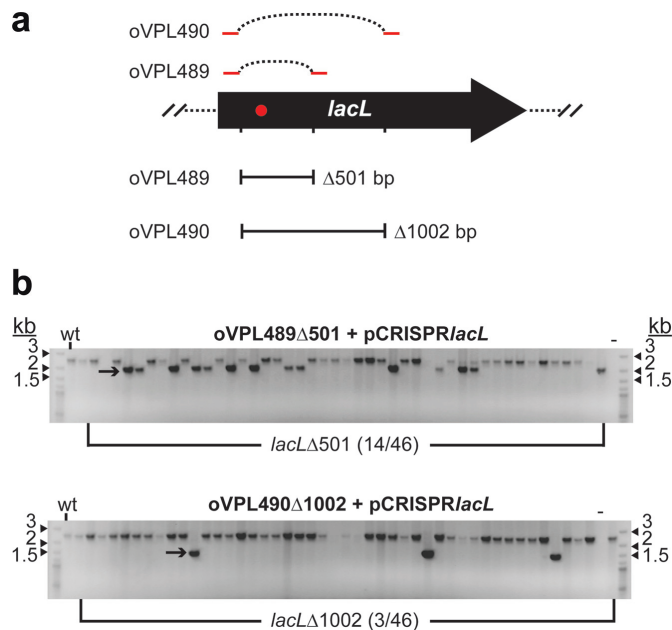


**Figure 3.** Identification of low-efficiency ssDNA recombineering events by CRISPR-Cas9 selection. (a) Experimental design to generate in-frame deletions of 501 and 1002 base pairs in the *L. reuteri lacL* locus by recombineering oligonucleotides oVPL489 $\Delta$ 501 and oVPL490 $\Delta$ 1002, respectively. The black arrow represents the *lacL* gene and the CRISPR-Cas9 target region is illustrated by a red dot. oVPL489 $\Delta$ 501 and oVPL490 $\Delta$ 1002, each a fusion of two 40 base lagging strand sequences (red lines), yield when incorporated deletions of 501 and 1002 bp, thereby also deleting the *lacL* protospacer target sequence. (b) PCR oligonucleotides flanking the target deletion sites generate amplicons of ~2.5 kb (wild-type sequence), 2 kb (*lacL* $\Delta$ 501) or 1.5 kb (*lacL* $\Delta$ 1002). With CRISPR-Cas9 selection, 30% (14/46) of screened colonies yielded amplicons of 2 kb indicative of incorporation of oVPL489 $\Delta$ 501 (top gel). Deletions of 1 kb were confirmed by PCR in 7% (3/46) of colonies indicative of incorporation of oVPL490 $\Delta$ 1002 (bottom gel). Data shown are representative images from three independent experiments.

that we used oligonucleotide oVPL578 $\Delta$ 702 combined with pCRISPR<sub>srtA</sub>. For screening purposes, we used oligonucleotides that flank *srtA* (oVPL468-oVPL469). In two independent experiments,  $8 \pm 0\%$  of the screened cells showed that oVPL578 $\Delta$ 702 was incorporated in the chromosome (data not shown). In conclusion, oligonucleotide-mediated deletions up to 1 kb are a realistic approach to edit the *L. reuteri* 6475 genome in a time-efficient manner when combined with CRISPR-Cas9 selection.

### Codon saturation mutagenesis by dual-step CRISPR-assisted recombineering

CRISPR-assisted recombineering opens up the exciting possibility to perform codon mutagenesis in the *L. reuteri* chromosome. In *L. reuteri*, non-homologous bases can be 10 bases from the proximal end in a 80-mer oligonucleotide (unpublished observations), meaning that the resulting mismatches can be as far as 60 bases apart. Therefore, one is not restricted to only the PAM site for mutagenesis. To show that CRISPR-Cas9-assisted recombineering is a viable approach for codon mutagenesis studies, we designed an oligonucleotide (oVPL627\_NNK) that has the following key features: (i) four adjacent non-homologous bases,

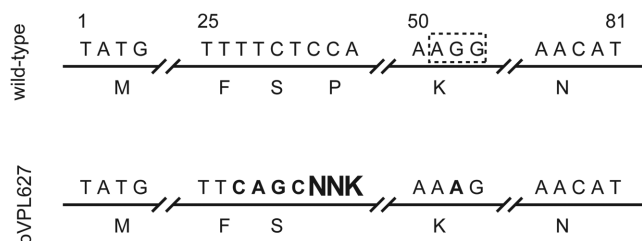


**Figure 4.** Oligonucleotide design for codon mutagenesis by means of CRISPR–Cas9-assisted recombineering. Fragments of the coding sequence of the sortase target region are shown. Sequences not shown are indicated with //. Numbers above the sequence indicate the relative base positions in the recombineering oligonucleotide. Below the triplet, located centrally, is the corresponding amino acid shown. The sequence boxed with a dashed line (AGG) represents that PAM sequence (top panel). The recombineering oligonucleotide oVPL627 is designed such that upon incorporation in the chromosome multiple base changes are made (all indicated in bold sequence). Incorporation of the non-homologous bases (position 27–30, and 52) yields silent mutations, but is predicted to evade the mismatch repair system and to modify the PAM site, respectively. A degenerate codon (NNK; N = A/T/G/C, K = G/T) at position 31–33 can result in 32 codons encoding 20 amino acids. Thus, incorporation of oVPL627 in the chromosome modifies the PAM sequence and will result in codon mutagenesis of a single codon.

which yield silent mutations, and are expected to evade the mismatch repair system; (ii) a single non-homologous base yielding a silent mutation, which modifies the NGG PAM motif; (iii) the presence of a degenerate triplet (NNK; N = A/T/G/C and K = G/T), which can result in 32 codons covering all 20 amino acids, but reduces the chance to incorporate a stop codon (Figure 4). Our experimental design was such that we modified the same PAM site that could be used in combination with pCRISPR<sub>srtA</sub>, and a dual-step approach was chosen to maximize the number of recombinants. We first transformed 100 µg oVPL627\_NNK, followed by transformation of 100 ng pCRISPR<sub>srtA</sub>. A total of 180 tetracycline-resistant colonies were screened by MAMA-PCR to identify recombinants. The MAMA oligonucleotide anneals to four adjacent bases, which are incorporated by oVPL627\_NNK, but its annealing is not dependent on the bases deduced from NNK. Approximately 50% of the screened colonies were confirmed to have incorporated oVPL627\_NNK (data not shown), and this percentage is comparable to what has been observed in *E. coli* when the PAM site is AAG (25). The pool of 91 recombinant colonies was subsequently used as template for a second PCR to generate 1-kb amplicons, which were submitted for DNA sequencing analysis. All 91 clones were confirmed to have a recombinant genotype, but five clones had a mutation in the oligonucleotide target region different than depicted by oVPL627\_NNK. These include two single base deletion events, and two single transition events in which a cytosine base was replaced by a thymine base. One clone showed seven modified adjacent bases as depicted by oVPL627\_NNK (position 25–32); however, the PAM site was not modified and was confirmed to be NGG. The remainder of 86 clones revealed that the triplet coding for proline at position 144 (P144) was replaced with base(s) yielding triplets that code for 19 amino acids other than proline, or the termination codon TAG (Table 1). Interestingly, looking at the nucleotide distribution of the various triplets

**Table 1.** Codon mutagenesis of SrtA P144

		2ND			
		T	C	A	G
1ST	T	2 TTT PHE 2 TTG LEU	0 TCT SER 0 TCG	3 TAT TYR 6 TAG STOP	4 TGT CYS 6 TGG TRP
	C	0 CTT LEU 0 CTG	0 CCT PRO 0 CCG	2 CAT HIS 1 CAG GLN	2 CGT ARG 5 CGG
A	A	1 ATT ILE 3 ATG MET	0 ACT THR 1 ACG	9 AAT ASN 8 AAG LYS	5 AGT SER 0 AGG ARG
	G	5 GTT VAL 3 GTG	2 GCT ALA 0 GCG	1 GAT ASP 4 GAG GLU	6 GGT GLY 5 GGG

#### nucleotide distribution

N		N		K	
T: 23	T: 16	T: 42			
C: 10	C: 3	G: 44			
A: 27	A: 34				
G: 26	G: 33				

Modified codon table showing only the triplets that could have been obtained by the degenerate codon NNK (N = A/T/G/C, K = G/T) upon incorporation of oVPL627 in the gene encoding sortase (SrtA), replacing the amino acid proline at position 144 (P144). The left column and the top row (both in gray boxes) indicate the first (1st) and second (2nd) nucleotide. Right of each triplet is the coding amino acid shown. Left of each triplet is the number of sequences shown that are retrieved from the pool of 86 recombinants. Below is the nucleotide distribution within the NNK codon shown based on the 86 recombinants obtained in our codon mutagenesis study.

derived from NNK, we noted that relatively few codons are obtained with the base cytosine at position 1 or 2 in the NNK codon, which are identical to the wild-type sequence. Despite an uneven distribution, our results show that codon saturation mutagenesis by means of CRISPR–Cas9-assisted recombineering is a realistic approach in *L. reuteri*.

## DISCUSSION

This work describes the development of CRISPR–Cas9 genome editing in combination with ssDNA recombineering in *L. reuteri* 6475 that allows identification of mutations at efficiencies up to 100%. We uncovered that co-transformation of a recombineering oligonucleotide and a CRISPR–target plasmid, a single-step approach, will yield recombinants when ssDNA recombineering efficiencies are optimal; however, these levels will not suffice to identify recombinants with an oligonucleotide that does not evade mismatch repair as 100-fold fewer recombinants may be obtained bringing it below the detection limit.

A dual-step approach increased the level of recombinants significantly and may be attributed to a variety of parameters, including the increased level of transformants obtained with the pCRISPR<sub>ctrl</sub> plasmid. The transformation efficiency of pCRISPR<sub>ctrl</sub> in *L. reuteri* 6475 was ~100-fold higher in the absence of RecT induction prior to transformation. We initially thought that high levels of RecT in cells

transformed with pCRISPR-derivatives were linked to the lower transformation efficiency we observed in the single-step procedure. Since pCRISPR<sub>ctrl</sub> is derived from a plasmid with a rolling-circle mode of replication (pSH71 origin), which generates ssDNA intermediates during replication (41), we hypothesized that RecT could bind and interfere with replication. We tested this by transforming a rolling circle and a theta replicating plasmid in *L. reuteri* wild-type or *L. reuteri* expressing RecT. However, each plasmid yielded comparable transformation efficiencies in each of the strains tested (data not shown), suggesting that parameters other than RecT contribute to the differences in transformation efficiency between the single-step and dual-step procedure. We also examined the possibility that the high oligonucleotide concentration would reduce the efficiency at which pCRISPR transformants, and thus recombinants, can be obtained in the single-step approach. Preliminary data showed that reducing the oligonucleotide concentration from 100 to 10  $\mu\text{g}$  increased the plasmid transformation efficiency by 4-fold, but only 2-fold more recombinants were obtained, whereas co-transformation of 1  $\mu\text{g}$  oligonucleotide did not improve the transformation efficiency and the level of recombinants. The latter can be attributed to the fact that significantly fewer recombinants are obtained with 1  $\mu\text{g}$  recombinering oligonucleotide compared to 100  $\mu\text{g}$  (15). Thus, fine-tuning the balance between oligonucleotide concentrations and pCRISPR only slightly improved the number of recombinants in the single-step approach.

A less pronounced, yet reproducible improvement with the dual-step approach may be attributed to the prolonged replication time when the recombinering oligonucleotide is in the cell prior to CRISPR–Cas9 selection. We see that relative to the pCRISPR<sub>ctrl</sub>, approximately 2-fold more putative recombinants are obtained compared to the single-step approach, suggesting that prolonged recovery may increase the number of cells in which the recombinering oligonucleotide is incorporated. This is in line with work published previously showing that a recombinering oligonucleotide targeting the *rpoB* gene yields 5-fold more recombinants when cells are grown in the absence of rifampicin selection compared to plating cells directly on selective plates after recovery of electroporation (15).

Although the dual-step procedure yielded a larger pool of recombinants, we also obtained cells that escaped the CRISPR–Cas9 selection. These escape mutants were obtained when cells with unmodified PAM sequence (within *lacL*) were transformed with pCRISPR<sub>lacL</sub>. Thus, cells survived, which should have been killed. Sequence analysis of the *lacL* region of 10 escaper colonies did not reveal a mutation in the protospacer or the PAM region in the chromosome (data not shown), suggesting that a mutation in either pCRISPR<sub>lacL</sub> or pVPL3004 could have attributed to the presence of the escaper colonies, as previously described for *E. coli* (25). The frequency of CRISPR–Cas9 survivors was calculated by determining the ratio between the number of cfu obtained from pCRISPR<sub>lacL</sub> / pCRISPR<sub>ctrl</sub>. Interestingly, this frequency in *L. reuteri* was determined to be  $2.5 \times 10^{-4}$ , identical to that observed in *E. coli*. This may suggest comparable mutation and recombination rates in these organisms, and that differences that exist in codon

usage between these strains do not affect CRISPR–Cas9 activity.

In addition to escapers, CRISPR–Cas9 has been shown to introduce double-strand breaks in off-target sites (42). Although we were able to select for mutations in different loci, we cannot rule out that a proportion of cells was killed due to off-target cleavage, even if the recombinering oligonucleotide was incorporated. From the population of cells that was transformed with plasmid DNA, ~1% of this population survived CRISPR selection. Since we showed that 90–100% of these survivor cells were confirmed to be a mutant genotype, we can conclude that ~1% of the total population of cells transformed are recombinant. These levels are comparable to what has been described previously for unselected ssDNA recombinering in *L. reuteri* (15). Thus, if off-target cleavage occurs, this will likely be at low frequencies for the loci described in this study.

To further exemplify the utility of CRISPR–Cas9-assisted recombinering, we also performed codon mutagenesis in the *L. reuteri* chromosome. With proper oligonucleotide design, the target sequence is not restricted to the PAM. In *L. reuteri* non-homologous bases can be present 10 bases from each proximal end in the oligonucleotide (unpublished observations). That means that for a 80-mer oligonucleotide, a 60-bp span is covered, and within that range mutations can be generated in the PAM, in addition to upstream and downstream located sequences. Analyses of the *L. reuteri* chromosome showed that NGG motifs are present every 15 base pairs. Thus, a single recombinering oligonucleotide would be able to cover multiple NGG PAM sites, and offers plenty opportunity to edit the chromosome.

In this study, we designed an oligonucleotide that is predicted to evade the mismatch repair system, incorporates a degenerate codon, and modifies the PAM sequence from NGG to NAG. A NAG PAM sequence in *E. coli* results in ~50% cleavage by Cas9 (25). We observed similar efficiencies in *L. reuteri* despite the fact that in addition to the modified PAM sequence up to seven adjacent non-homologous bases were present in the protospacer at position 17–23 (position 1 being the first nucleotide upstream of NGG). These results suggest that the presence of the seven non-homologous bases in this location of the protospacer do not affect Cas9 cleavage. Although Jiang *et al.* did not investigate the role of multiple adjacent mismatches in the protospacer on Cas9 cleavage, their results also suggest that single base changes at position 13–20 in the protospacer do not affect Cas9 cleavage (25). Ran *et al.* showed that the *S. pyogenes* CRISPR–Cas9 system cleaves target DNA efficiently if non-homologous bases at position 21–28 are present in the protospacer, whereas a protospacer of 17 base pairs still yields efficient targeting by Cas9 (43,44). Collectively, it is therefore plausible that non-homologous bases in the protospacer at position 17–23 do not affect the efficacy at which Cas9 cleaves the *L. reuteri* chromosome.

Sequence analysis of 86 recombinants revealed that a single triplet encoding proline was modified to yield 19 different amino acids. We observed that the abundance of recombinant sequences was not evenly distributed as some triplets were not recovered (like CTT), whereas as many as nine AAT triplets were recovered from the pool of 86 recombinants. A closer look at the nucleotide distribution within

the triplets derived from the NNK codons in 86 clones revealed that only three codons were recovered in which the middle base is a cytosine, which interestingly is identical to the wild-type sequence. We do not know the rationale for this, but possibly the efficacy by which oligonucleotides are incorporated in the *L. reuteri* is lower when a single homologous base is flanked by mismatched base(s). It thus cannot be ruled out that the efficacy of ssDNA recombineering may be sequence context-dependent. For example, previously in *L. reuteri* ssDNA recombineering, efficiencies varied in different targets from 0.4% up to as high as 19% (15). Although we were successful in codon-saturation mutagenesis in the *L. reuteri* chromosome, improved molecular insights into off-target cleavage, and sequence-dependent ssDNA recombineering will be useful when technologies like CRISPR–Cas9 and ssDNA recombineering are applied to generate whole genome mutant libraries. Also, although we were able to cure all plasmids combined after ~70 generations in at least 30% of the cell population in three independent clones (data not shown), the development of a temperature sensitive replicon for pCRISPR may further improve the efficacy of plasmid curing since pCRISPR appears most stable in *L. reuteri* 6475 compared to pVPL3004 and pVPL3017.

The ability to select for recombinant cells by CRISPR–Cas9 allowed for selection of oligonucleotide-mediated chromosomal deletions up to 1 kb, which has not been previously described in *Firmicutes*. The use of CRISPR–Cas9 to identify mutations that occur at low frequencies opens up the possibility to expand this selection approach to organisms with industrial and medical relevance with low efficiency engineering tools, including various lactobacilli and the majority of bifidobacteria. Also, our work combined with current developments in CRISPR–Cas9 genome editing makes the application of MAGE in lactobacilli and bifidobacteria tantalizing, yet not unreasonable (45,46). CRISPR–Cas9 may also complement more mainstream genetic approaches to engineer genomes, such as double crossover strategies to delete or insert genes. The protospacer may be designed such that only cells will be recovered if the deletion or insertion event has taken place, thereby eliminating unedited cells. Taken together, CRISPR–Cas9 selection combined with genetic engineering tools such as ssDNA recombineering provides researchers with a toolset that widens the horizon of fine-tuned genome editing in a variety of organisms.

## SUPPLEMENTARY DATA

[Supplementary Data](#) are available at NAR Online.

## ACKNOWLEDGMENTS

We thank Jim Steele, Heidi Goodrich-Blair and Lothar Steidler for reading the manuscript, and Robert Britton, Jade Wang and Rodolphe Barrangou for discussions.

## FUNDING

Startup funds from University of Wisconsin-Madison [to J.P.V.P.]. Funding for open access charge: University of Wisconsin-Madison [to J.P.V.P.].

*Conflict of interest statement.* None declared.

## REFERENCES

- König,H. and Fröhlich,J. (2009) Lactic acid bacteria. In: König,H., Fröhlich,J. and Uden,G. (eds) *Biology of Microorganisms on Grapes, in Must and in Wine*. Springer, Berlin, Heidelberg, pp. 3–29.
- Aureli,P., Capurso,L., Castellazzi,A.M., Clerici,M., Giovannini,M., Morelli,L., Poli,A., Pregliasco,F., Salvini,F. and Zuccotti,G.V. (2011) Probiotics and health: an evidence-based review. *Pharmacolog. Res.*, **63**, 366–376.
- Vaghef-Mehrabany,E., Alipour,B., Homayouni-Rad,A., Sharif,S.-K., Asghari-Jafarabadi,M. and Zavvari,S. (2014) Probiotic supplementation improves inflammatory status in patients with rheumatoid arthritis. *Nutrition*, **30**, 430–435.
- Ljungh,A. and Wadström,T. (2006) Lactic acid bacteria as probiotics. *Curr. Issues Intest. Microbiol.*, **7**, 73–89.
- Clarke,G., Cryan,J.F., Dinan,T.G. and Quigley,E.M. (2012) Review article: probiotics for the treatment of irritable bowel syndrome—focus on lactic acid bacteria. *Aliment. Pharmacol. Ther.*, **35**, 403–413.
- G-Alegria,E., López,I., Ruiz,J.I., Sáenz,J., Fernández,E., Zarazaga,M., Dízy,M., Torres,C. and Ruiz-Larrea,F. (2004) High tolerance of wild *Lactobacillus plantarum* and *Oenococcus oeni* strains to lyophilisation and stress environmental conditions of acid pH and ethanol. *FEMS Microbiol. Lett.*, **230**, 53–61.
- Steidler,L., Hans,W., Schotte,L., Neiryneck,S., Obermeier,F., Falk,W., Fiers,W. and Remaut,E. (2000) Treatment of murine colitis by *Lactococcus lactis* secreting interleukin-10. *Science*, **289**, 1352–1355.
- Daniel,C., Roussel,Y., Kleerebezem,M. and Pot,B. (2011) Recombinant lactic acid bacteria as mucosal biotherapeutic agents. *Trends Biotechnol.*, **29**, 499–508.
- Lucena,B.T.L., Santos dos,B.M., Moreira,J.L., Moreira,A.P.B., Nunes,A.C., Azevedo,V., Miyoshi,A., Thompson,F.L. and de Moraes,M.A. (2010) Diversity of lactic acid bacteria of the bioethanol process. *BMC Microbiol.*, **10**, 298–305.
- Teusink,B. and Smid,E.J. (2006) Modelling strategies for the industrial exploitation of lactic acid bacteria. *Nat. Rev. Microbiol.*, **4**, 46–56.
- Bron,P.A. and Kleerebezem,M. (2011) Engineering lactic acid bacteria for increased industrial functionality. *Bioeng. Bugs*, **2**, 80–87.
- Sybesma,W., Burgess,C., Starrenburg,M., van Sinderen,D. and Hugenholtz,J. (2004) Multivitamin production in *Lactococcus lactis* using metabolic engineering. *Metab. Eng.*, **6**, 109–115.
- Gaspar,P., Neves,A.R., Ramos,A., Gasson,M.J., Shearman,C.A. and Santos,H. (2004) Engineering *Lactococcus lactis* for production of mannitol: high yields from food-grade strains deficient in lactate dehydrogenase and the mannitol transport system. *Appl. Environ. Microbiol.*, **70**, 1466–1474.
- Wegkamp,A., de Vos,W.M. and Smid,E.J. (2009) Folate overproduction in *Lactobacillus plantarum* WCFS1 causes methotrexate resistance. *FEMS Microbiol. Lett.*, **297**, 261–265.
- van Pijkeren,J.P. and Britton,R.A. (2012) High efficiency recombineering in lactic acid bacteria. *Nucleic Acids Res.*, **40**, e76.
- van Pijkeren,J.P., Neoh,K.M., Sirias,D., Findley,A.S. and Britton,R.A. (2012) Exploring optimization parameters to increase ssDNA recombineering in *Lactococcus lactis* and *Lactobacillus reuteri*. *Bioengineered*, **3**, 209–217.
- Lim,S.I., Min,B.E. and Jung,G.Y. (2008) Lagging strand-biased initiation of red recombination by linear double-stranded DNAs. *J. Mol. Biol.*, **384**, 1098–1105.
- Ellis,H.M., Yu,D., DiTizio,T. and Court,D.L. (2001) High efficiency mutagenesis, repair, and engineering of chromosomal DNA using single-stranded oligonucleotides. *Proc. Natl Acad. Sci. U.S.A.*, **98**, 6742–6746.
- Costantino,N. and Court,D.L. (2003) Enhanced levels of lambda Red-mediated recombinants in mismatch repair mutants. *Proc. Natl Acad. Sci. U.S.A.*, **100**, 15 748–15 753.
- Sawitzke,J.A., Costantino,N., Li,X.-T., Thomason,L.C., Bubunenko,M., Court,C. and Court,D.L. (2011) Probing cellular processes with oligo-mediated recombination and using the knowledge gained to optimize recombineering. *J. Mol. Biol.*, **407**, 45–59.

21. Huen, M.S.Y., Li, X.-T., Lu, L.-Y., Watt, R.M., Liu, D.-P. and Huang, J.-D. (2006) The involvement of replication in single stranded oligonucleotide-mediated gene repair. *Nucleic Acids Res.*, **34**, 6183–6194.
22. Datta, S., Costantino, N., Zhou, X. and Court, D.L. (2008) Identification and analysis of recombineering functions from Gram-negative and Gram-positive bacteria and their phages. *Proc. Natl Acad. Sci. U.S.A.*, **105**, 1626–1631.
23. van Kessel, J.C. and Hatfull, G.F. (2007) Recombineering in *Mycobacterium tuberculosis*. *Nat. Methods*, **4**, 147–152.
24. Gerlach, R.G., Jäckel, D., Hölzer, S.U. and Hensel, M. (2009) Rapid oligonucleotide-based recombineering of the chromosome of *Salmonella enterica*. *Appl. Environ. Microbiol.*, **75**, 1575–1580.
25. Jiang, W., Bikard, D., Cox, D., Zhang, F. and Marraffini, L.A. (2013) RNA-guided editing of bacterial genomes using CRISPR-Cas systems. *Nat. Biotechnol.*, **31**, 233–239.
26. Horvath, P. and Barrangou, R. (2010) CRISPR/Cas, the immune system of bacteria and archaea. *Science*, **327**, 167–170.
27. Wiedenheft, B., Sternberg, S.H. and Doudna, J.A. (2012) RNA-guided genetic silencing systems in bacteria and archaea. *Nature*, **482**, 331–338.
28. Barrangou, R. (2013) CRISPR-Cas systems and RNA-guided interference. *Wiley Interdiscip. Rev. RNA*, **4**, 267–278.
29. Sander, J.D. and Joung, J.K. (2014) CRISPR-Cas systems for editing, regulating and targeting genomes. *Nat. Biotechnol.*, **32**, 347–355.
30. Chylinski, K., Le Rhun, A. and Charpentier, E. (2013) The tracrRNA and Cas9 families of type II CRISPR-Cas immunity systems. *RNA Biol.*, **10**, 726–737.
31. Britton, R.A., Irwin, R., Quach, D., Schaefer, L., Zhang, J., Lee, T., Parameswaran, N. and McCabe, L.R. (2014) Probiotic *L. reuteri* treatment prevents bone loss in a menopausal ovariectomized mouse model. *J. Cell Physiol.*, doi:10.1002/jcp.24636.
32. Spinler, J.K., Taweechoatipatr, M., Rognerud, C.L., Ou, C.N., Tumwasorn, S. and Versalovic, J. (2008) Human-derived probiotic *Lactobacillus reuteri* demonstrate antimicrobial activities targeting diverse enteric bacterial pathogens. *Anaerobe*, **14**, 166–171.
33. Thomas, C.M., Hong, T., van Pijkeren, J.P., Hemarajata, P., Trinh, D.V., Hu, W., Britton, R.A., Kalkum, M. and Versalovic, J. (2012) Histamine derived from probiotic *Lactobacillus reuteri* suppresses TNF via modulation of PKA and ERK signaling. *PLoS One*, **7**, e31951.
34. Lin, Y.P., Thibodeaux, C.H., Peña, J.A., Ferry, G.D. and Versalovic, J. (2008) Probiotic *Lactobacillus reuteri* suppress proinflammatory cytokines via c-Jun. *Inflamm. Bowel Dis.*, **14**, 1068–1083.
35. Eaton, K.A., Honkala, A., Auchtung, T.A. and Britton, R.A. (2011) Probiotic *Lactobacillus reuteri* ameliorates disease due to enterohemorrhagic *Escherichia coli* in germfree mice. *Infect. Immun.*, **79**, 185–191.
36. Holo, H. and Nes, I.F. (1989) High-frequency transformation, by electroporation, of *Lactococcus lactis* subsp. *cremoris* grown with glycine in osmotically stabilized media. *Appl. Environ. Microbiol.*, **55**, 3119–3123.
37. Ahrné, S., Molin, G. and Axelsson, L. (1992) Transformation of *Lactobacillus reuteri* with electroporation: studies on the erythromycin resistance plasmid pLUL631. *Curr. Microbiol.*, **24**, 199–205.
38. Josson, K., Scheirlinck, T., Michiels, F., Platteeuw, C., Stanssens, P., Joos, H., Dhaese, P., Zabeau, M. and Mahillon, J. (1989) Characterization of a gram-positive broad-host-range plasmid isolated from *Lactobacillus hilgardii*. *Plasmid*, **21**, 9–20.
39. Gibson, D.G., Young, L., Chuang, R.-Y., Venter, J.C., Hutchison, C.A. and Smith, H.O. (2009) Enzymatic assembly of DNA molecules up to several hundred kilobases. *Nat. Methods*, **6**, 343–345.
40. Cha, R.S., Zarbl, H., Keohavong, P. and Thilly, W.G. (1992) Mismatch amplification mutation assay (MAMA): application to the c-H-ras gene. *PCR Methods Appl.*, **2**, 14–20.
41. Khan, S.A. (2000) Plasmid rolling-circle replication: recent developments. *Mol. Microbiol.*, **37**, 477–484.
42. Cho, S.W., Kim, S., Kim, Y., Kweon, J., Kim, H.S., Bae, S. and Kim, J.-S. (2014) Analysis of off-target effects of CRISPR/Cas-derived RNA-guided endonucleases and nickases. *Genome Res.*, **24**, 132–141.
43. Ran, F.A., Hsu, P.D., Lin, C.-Y., Gootenberg, J.S., Konermann, S., Trevino, A.E., Scott, D.A., Inoue, A., Matoba, S., Zhang, Y. *et al.* (2013) Double nicking by RNA-guided CRISPR Cas9 for enhanced genome editing specificity. *Cell Regen.*, **154**, 1380–1389.
44. Fu, Y., Sander, J.D., Reyon, D., Cascio, V.M. and Joung, J.K. (2014) Improving CRISPR-Cas nuclease specificity using truncated guide RNAs. *Nat. Biotechnol.*, **32**, 279–284.
45. Cong, L., Ran, F.A., Cox, D., Lin, S., Barretto, R., Habib, N., Hsu, P.D., Wu, X., Jiang, W., Marraffini, L.A. *et al.* (2013) Multiplex genome engineering using CRISPR/Cas systems. *Science*, **339**, 819–823.
46. Wang, H.H., Isaacs, F.J., Carr, P.A., Sun, Z.Z., Xu, G., Forest, C.R. and Church, G.M. (2009) Programming cells by multiplex genome engineering and accelerated evolution. *Nature*, **460**, 894–898.